2018 International Symposium on Electromagnetic Compatibility - EMC EUROPE, 27-30 August, 2018

Design and Evaluation of a Broadband Source Stirring Antenna for use in a Reverberation Chamber

Andy C Marvin
Dept of Electronic Engineering
University of York
York, UK
andy.marvin@york.ac.uk

Liam Franks
Dept of Electronic Engineering
University of York
York, UK

Ian Flintoft
Dept of Electronic Engineering
University of York
York, UK

John Dawson
Dept of Electronic Engineering
University of York
York, UK
john.dawson@york.ac.uk

Martin Robinson
Dept of Electronic Engineering
University of York
York, UK
martin.robinson@york.ac.uk

***Abstract*—a new broad-band antenna structure specifically designed for antenna position stirring in a reverberation chamber is described. The antenna features a reactive rotating source coupler that overcomes the problems of cable and connector reliability and stability often encountered in antenna source stirring due to cable movement. The stirring performance of the new antenna is evaluated by observation of the reduction in Rician K-factor facilitated by the antenna.**

Keywords—; reverberation chamber, source stirring, antenna

I. Introduction

The most common way of mechanical stirring in a reverberation chamber used for EMC measurements is the use of a rotating stirrer to provide the changing boundary conditions required of the stirring process. Other possibilities for mechanical stirring are to move the equipment-under-test (EUT) on a platform or to move the measurement antennas – source stirring. This latter technique is the subject of this paper.

The principal problems with antenna source stirring are the reliability and stability of the cables and connections as the antenna is moved. Here we describe a proof-of-concept antenna structure that overcomes this problem. The structure comprises a broadband antenna operating in the 2GHz to 8.5GHz frequency range. This frequency range was chosen for experimental convenience and could be extended if required. The antenna is moved by rotation about its feed-point where energy is reactively coupled into the antenna. The phase centre of the antenna is maintained at a radius from the rotation point of at least one wavelength. In this demonstration antenna the antenna is rotated through an angle of 180º, an angle defined by mechanical construction constraints. Assuming a one wavelength radius of rotation, the phase centre thus moves over a distance of π wavelengths, sufficient for an estimated minimum of ten independent antenna positions [1]. In principle the antenna rotation could provide sufficient stirring to operate the chamber correctly. In this proof-of-concept antenna the antenna is operated in conjunction with a conventional rotating mechanical stirrer. The effectiveness of the antenna is demonstrated by observation of the Rician K-factor with and without antenna movement.

II. Antenna Design

The basic antenna design is an exponentially tapered transmission line structure operating over a ground-plane. The structure is designed to maintain a 50Ohm characteristic impedance of the transmission line throughout the taper. Images of the antenna are shown in Fig 1.

The brass tapered transmission line is supported by the Perspex structure shown. It rotates about the centre of the lower gear wheel. The upper gear wheel is driven by a

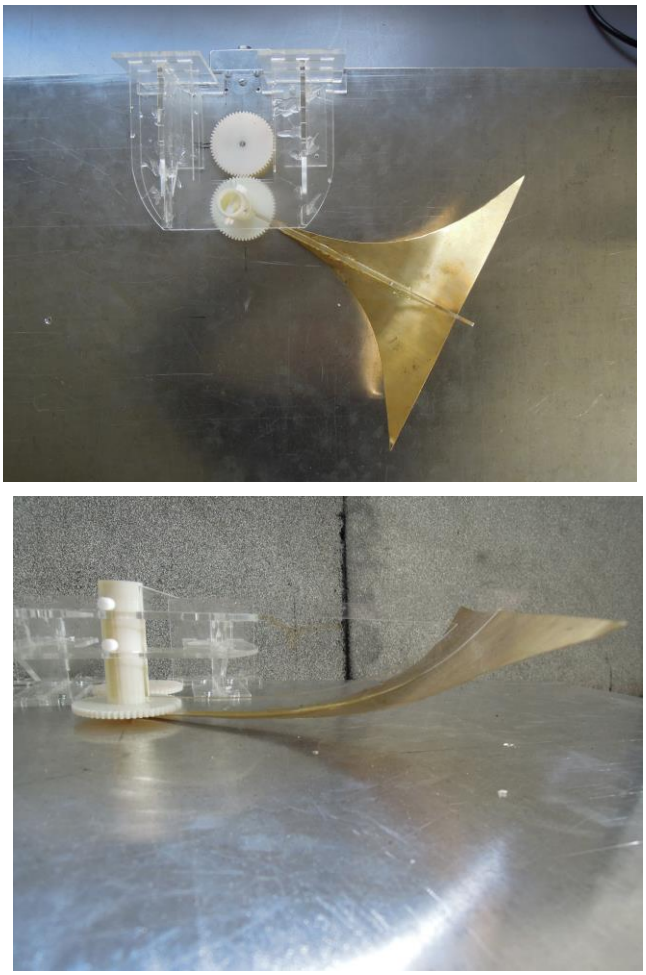

Fig 1 Images of the completed antenna.

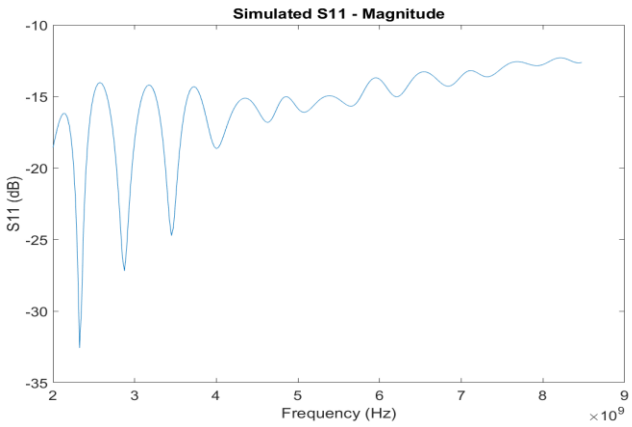

Fig 2 Simulated reflection coefficient of the antenna, 2GHz -8.5GHz

stepper motor under the ground-plane. The ratio of the exponential antenna element width to its height above the ground-plane is a constant. The maximum width of the tapered transmission line is 250mm and its maximum height above the ground-plane is 70mm. The radius of rotation of the antenna at its maximum width is 200mm.

The structure was simulated using the boundary element code CONCEPT [2] to verify its performance. Fig 2 shows the simulated input reflection coefficient S11 indicating that the basic antenna structure maintains a good impedance match (S11 smaller than -10dB) over the frequency range 2GHz to 8.5GHz.

The antenna is fed at its centre of rotation. The extended centre conductor of an SMA coaxial socket protrudes through the ground-plane and into a 10mm length of semi-rigid coaxial cable to form a reactive coupling element. This is not incorporated into the CONCEPT simulation of the antenna. An image of the dismantled feed point is shown in Fig3 which shows the outer of the coaxial section at the feed end of the tapered transmission line.

The CONCEPT derived input impedance data was modified by including the reactance of the transmission line feed segment in series and the input reflection coefficient of the complete antenna was calculated. This is compared to the

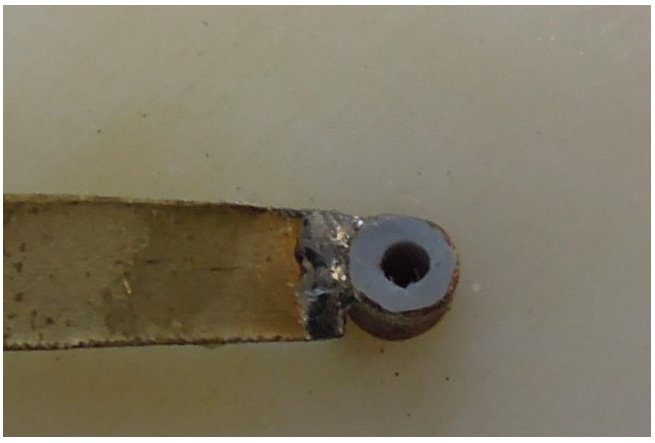

Fig 3 Antenna feed point with coaxial section.

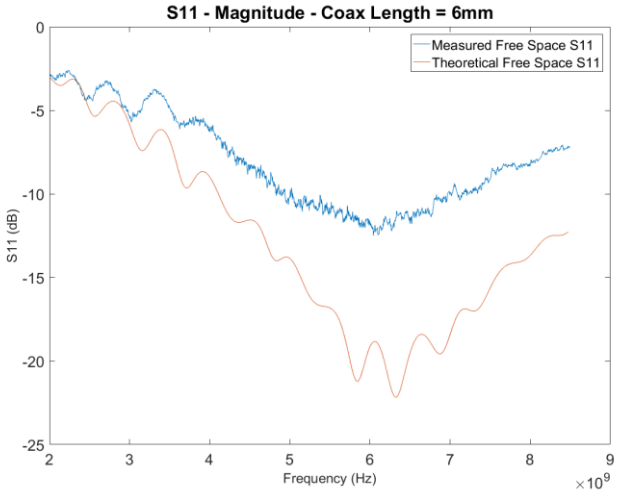

Fig 4. Comparison of simulated and measured reflection coefficients.

measured input reflection coefficient derived from the phasor average input reflection coefficient measured in the reverberation chamber in Fig 4. The annotation 6mm in this result indicates the best match between measurement and simulation. The actual penetration of the extended centre conductor was 10mm. The discrepancy is not yet explained. This phasor average reflection coefficient measured in the reverberation chamber is equivalent to the free-space reflection coefficient. For this measurement, the antenna was static and the mechanical stirrer was rotated to provide the samples for averaging. The antenna as measured maintains an adequate input reflection coefficient over the design frequency range.

The requirement to have a radius of rotation of at least one wavelength was demonstrated by CONCEPT simulation of the phase centre position of the completed antenna. The technique used for this relies on the inverse distance relationship between the phase centre to measurement point distance and the radiated field when the antenna's radiated field is observed in the radiating far-field. The antenna radiates principally along the direction of the transmission line. The radiated electric field was computed a range of distances in front of the antenna.

The reciprocal of this field was then plotted against distance from the antenna feed-point. The intercept of the resultant straight line on the distance axis is the phase centre radius from the feed-point. Fig 5 shows a typical regression plot for evaluating the phase centre at 5GHz. The linear relationship between the inverse field strength and the evaluation point to feed point distance indicates that radiating far-field conditions are maintained.

Fig 6 shows the computed phase centre positions relative to the feed-point over the frequency range from 2GHz to 8.5GHz for six sets of distances from the feed point. The curve marked wavelength shows the wavelength for each frequency. In general, the phase centre to feed-point distance is in excess of the specified one wavelength.

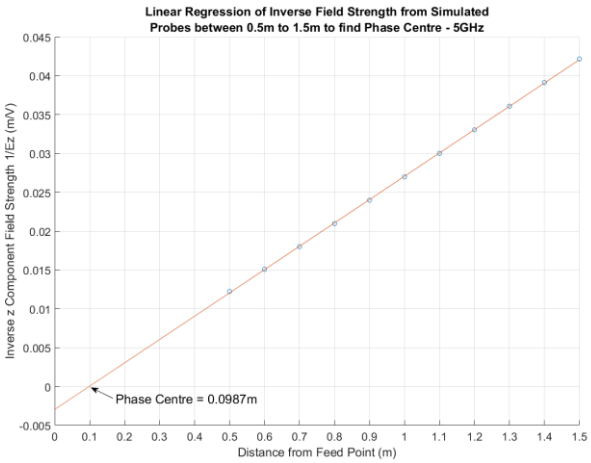

Fig 5. Phase centre regression plot at 5GHz.

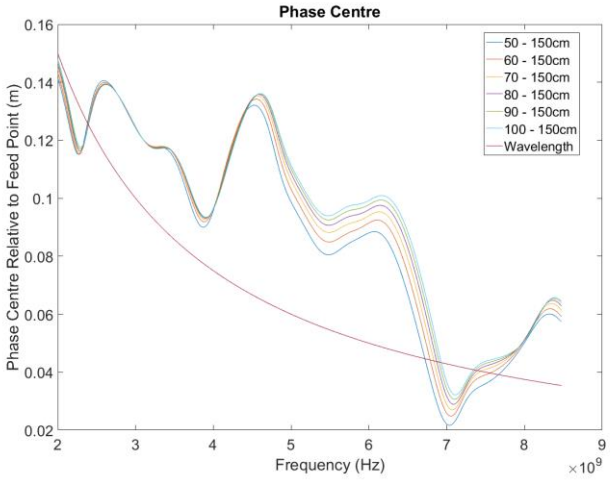

Fig 6. Simulated phase centre position.

III. ANTENNA TESTING

This proof of concept antenna is designed for use in a reverberation chamber alongside a conventional mechanical stirrer. The chamber used for testing has dimensions of 4.7m x 3m x 2.7m and is equipped with a rotating stirrer optimized for use in this chamber [3]. Its lowest usable frequency is 200MHz as defined by the IEC standard [1].

The technique chosen to demonstrate the antenna's efficacy was observation of the Rician K-factor in the chamber. The K-factor is the ratio of unstirred (stationary) to stirred received power in the chamber. In an ideal chamber there should be no unstirred power and the K-factor should be zero. The statistics of the magnitude of a single field component measured at each stirrer position in this case follow a Rayleigh distribution. Where unstirred power is present, the field statistics follow a Rician distribution. This power ratio is usually expressed in deciBels, and a K-factor of -20dB (0.01) represents a well stirred chamber. In practice a K-factor below -10dB can be considered adequate for EMC measurements.

The K-factors of the chamber with the source stirred antenna at a set of single positions was measured. This is then compared with the K-factor of the combination of rotating stirrer and rotated source stirred antenna.

To evaluate both the stirred and the un-stirred power transmitted between two antennas in the chamber a Vector Network Analyser is used to measure the complex (phasor) S21 transmission between the two antennas for each position of the stirrer or, in the case of the stirrer and the rotating antenna, for each combination of stirrer and antenna positions. This is done for each frequency.

In an ideal chamber with a K-factor of zero at a single frequency, the phasor average of the S21 values over all stirrer positions or position combinations should be zero. In a real chamber the phasor average will be non-zero. The square of the modulus this phasor average value is the unstirred power.

The stirred power is evaluated by centering the S21 values on the origin of the complex plane by subtracting the phasor average from each measured S21 value. The average of the moduli of these centered S21 values is squared to give the average stirred power.

The K-factor varies rapidly with frequency over a wide range. This is due to the values of the stirred power and the unstirred power being dependent on the phasor summation of multiple waves propagating over paths many wavelengths long within the chamber. Thus evaluating any changes in the K-factor over a frequency range is not possible from simple observation of a K-factor against frequency plot.

This is illustrated in Fig 7.where the frequency dependent K-factor is plotted for a typical case where the two antennas in the chamber are hidden one from another by the mechanical stirrer. There are 1601 frequency points between 2GHz and 8.5GHz. The K-factor varies over a range in excess of 60dB. In order to facilitate easier data evaluation the Probability Density Function (PDF) of the measured K-factors has been used in this work. A Kernel Distribution [4] was used to obtain a continuous estimation of each PDF.

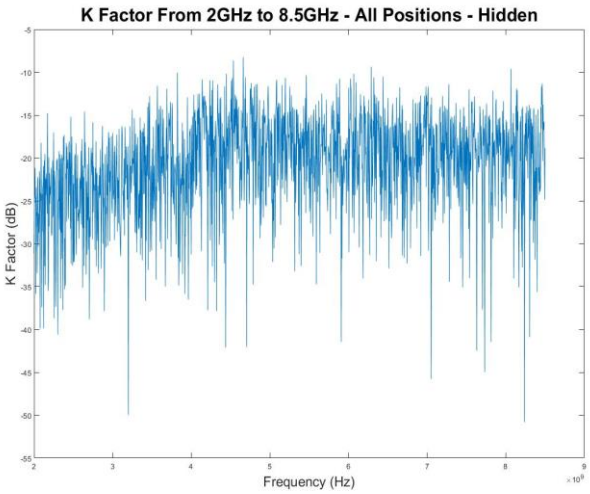

Fig 7. K-factor for stirrer and antenna rotated – 2GHz to 8.5GHz

IV. RESULTS

In each test the mechanical stirrer was moved over a complete rotation with fifty discrete positions. The stirred antenna was rotated over 180° with twenty discrete positions. Thus when both were used in combination one thousand stirrer positions were recorded at each of the 1601 frequency points between 2GHz and 8.5GHz.

A. Source and Receiving antennas hidden one from another

In the first set of tests the two antennas were hidden one from another by being placed on either side of the mechanical stirrer. This positioning should give the optimum K-factor as the unstirred power is reduced by the absence of a direct line-of-sight path between the two antennas. The residual unstirred power is due to stationary coupling paths between the antennas from single or multiple wall reflections that do not pass through the stirrer swept volume [5].

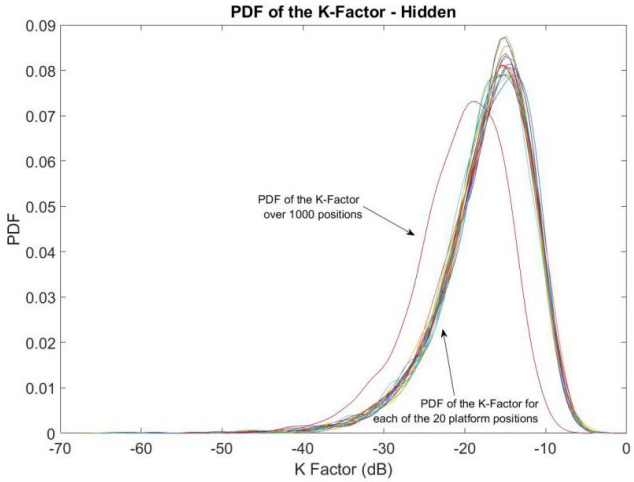

Fig 8. PDFs of K-factors for the hidden antenna combination.

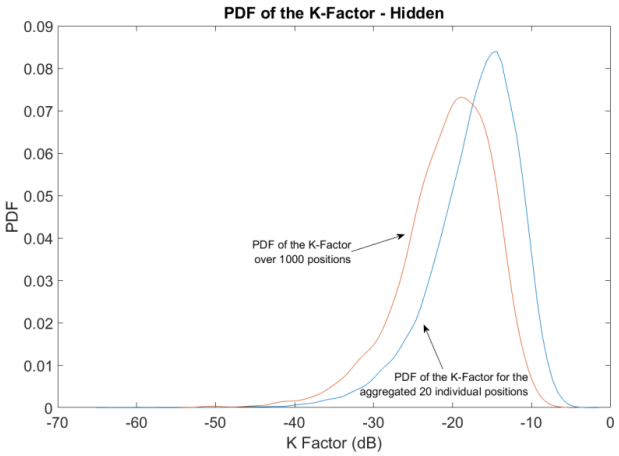

Fig 9. Aggregated K-factor of the twenty individual antenna positions compared to the composite K-factor for hidden antennas.

In Fig 8 the PDFs of the individual K-factors between 2GHz and 8.5GHz are plotted for each of the twenty antenna rotation positions along with the resultant PDF of the combined stirring of both the antenna and the stirrer with a total of one thousand positions. Each of the twenty PDFs for the discrete positions of the stirred antenna has an expectation value of around -14dB. The expectation value of the aggregated K-factors is around -19dB.Fig.9 shows the comparison of the PDFs where the twenty individual stirred antenna positions are aggregated into a single PDF.

B. Source and Receiving antennas in line-of-site

The second test was with the two antennas in the working volume of the chamber with a direct line-of-site path between them. In these circumstances the K-factors are expected to be larger. Fig 10 shows the aggregated K-factors of the twenty antenna positions along with the PDF of the combined antenna and stirrer rotation. The result is similar to that when the antennas are hidden one from another except that the K-factors are higher.
In this case the combined stirring gives an improvement in K-factor of 3dB with a reduction of the expectation value from -12.5dB to -15.5dB.

V. CONCLUSIONS

In this paper we have demonstrated a new proof of concept antenna structure that facilitates source antenna stirring as a supplement to a conventional rotating stirrer in a reverberation chamber. The antenna demonstrates a significant reduction in the Rician K-factor for the chamber when it is used alongside a conventional rotating stirrer. In the case where the source and receiving antennas are hidden one from another it is expected that the K-factor should be adequate as demonstrated. The improvement to the K-factor in this case resulting from the source antenna stirring of 5dB represents a factor three reduction in the unstirred power, a

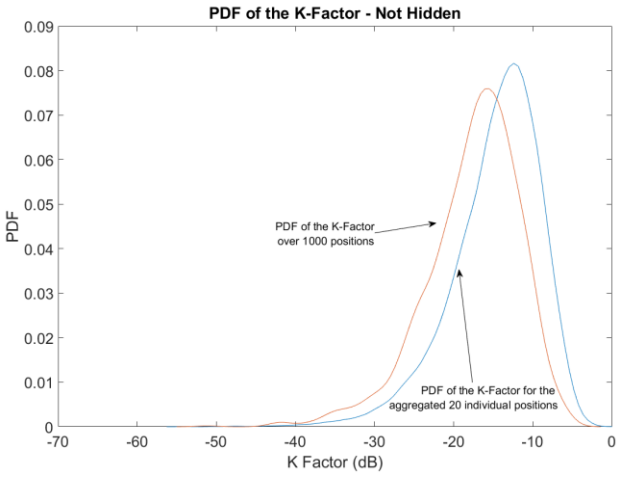

Fig 10. Aggregated K-factor of the twenty individual antenna positions compared to the combined K-factor for not hidden antennas.

significant result. In the case of the two antennas being in the working volume of the chamber, where larger K-factors are to be expected due to the line-of-sight path between the antennas, the 3dB reduction in K-factor obtained when the source antenna is rotated along with the rotating stirrer represents a halving of the unstirred power.

The radius of rotation of the antenna is a minimum of one wavelength over most of the frequency range. This was a target value for the proof of concept antenna. More efficient stirring could be achieved by increasing the radius through extending the tapered transmission line with a constant impedance section between the reactive feed point and the active part of the antenna. The increased radius of rotation of the antenna would increase the number of independent sample positions available. Such an antenna may facilitate adequate stirring without the use of a conventional stirrer.

REFERENCES

[1] International Electrotechnical Commission, 61000-4-21 ELECTROMAGNETIC COMPATIBILITY (EMC), Part 4:Testing and Measurement Techniques, Section21: Reverberation Chamber Test Methods

[2] CONCEPT-II, ver. 12.0, Hamburg University of Technology (TUHH), Hamburg.

[3] J Clegg, A.C. Marvin J.F.Dawson & S.J. Porter. "Optimisation of Stirrer Designs in a Reverberation Chamber." IEEE Transactions on Electromagnetic Compatibility. Vol 47, No 4 pp 824-832. Nov 2005.

[4] MathWorks, *Kernel Distribution*, uk.mathworks.com. Available:https://uk.mathworks.com/help/stats/kernel-distribution.html

[5] R J Pirkl, J M Ladbury & K A Remley, "The Reverberation Chamber's Unstirred Field: A Validation of the Image Theory Interpretation" IEEE International Symposium on EMC. Long Beach Florida, Aug 14-19, 2011.